MITSUBISHI ELECTRIC RESEARCH LABORATORIES
http://www.merl.com

Fingerprinting-Based Indoor Localization with Commercial MMWave WiFi - Part I: RSS and Beam Indices

Pajovic, M.; Wang, P.; Koike-Akino, T.; Sun, H.; Orlik, P.V.

TR2019-141 December 09, 2019

Abstract

Millimeter-wave (mmWave) communications is an emerging technology expected to bring unprecedented data rates and throughput. WiFi operating at unlicensed 60 GHz range is envisioned to become an ubiquitous technology and the IEEE 802.11ad standard is an initial attempt in that direction. Although spatial and temporal resolution of mmWave signals make them suitable for location estimation, a variety of hardwarerelated issues and commonly encountered difficulties in extracting channel measurements from commercial chipsets, challenge opportunistic use of commercial mmWave WiFi chips for indoor localization. We propose in this paper an indoor localization method that fingerprints transmit beam indices that a pair of WiFi transceivers employ to establish a mmWave link, as well as the resulting received signal strength (RSS). In particular, we develop an algorithm that learns possible probabilistic models from the fingerprint data and leverages them to perform indoor localization in the online stage. The proposed algorithm is experimentally evaluated using commercial 60 GHz WiFi routers in an office space

IEEE Global Communications Conference (GLOBECOM)

Fingerprinting-Based Indoor Localization with Commercial MMWave WiFi – Part I: RSS and Beam Indices

Milutin Pajovic[1], Pu Wang[1], Toshiaki Koike-Akino[1], Haijian Sun[2], Philip V. Orlik[1]
[1]Mitsubishi Electric Research Laboratories (MERL), Cambridge, MA, 02139, USA
[2]Utah State University, Logan, UT, 84322, USA

***Abstract*—Millimeter-wave (mmWave) communications is an emerging technology expected to bring unprecedented data rates and throughput. WiFi operating at unlicensed 60 GHz range is envisioned to become an ubiquitous technology and the IEEE 802.11ad standard is an initial attempt in that direction. Although spatial and temporal resolution of mmWave signals make them suitable for location estimation, a variety of hardware-related issues and commonly encountered difficulties in extracting channel measurements from commercial chipsets, challenge opportunistic use of commercial mmWave WiFi chips for indoor localization. We propose in this paper an indoor localization method that fingerprints transmit beam indices that a pair of WiFi transceivers employ to establish a mmWave link, as well as the resulting received signal strength (RSS). In particular, we develop an algorithm that learns possible probabilistic models from the fingerprint data and leverages them to perform indoor localization in the online stage. The proposed algorithm is experimentally evaluated using commercial 60 GHz WiFi routers in an office space area and localization error of around 30 cm is demonstrated.**

I. Introduction

Indoor localization, aimed to estimate location of people and objects in an enclosed area where signals from the Global Positioning System (GPS) do not penetrate, has received considerable attention over the last few decades. A variety of technologies such as radio (WiFi, infrared, RFID, ultra wideband, Zigbee, Bluetooth, DTV, cellular, FM), optics (lasers, cameras), sound (audible, ultrasound), magnetism (geomagnetism, coil-induced magnetism) have been considered to aid indoor localization. Leveraging one or more signal features that contain information about location, such as time (time of arrival, time of flight, time difference of arrival, round trip time), phase (phase of arrival, phase difference), angle of arrival or power (received signal strength, signal to noise ratio) has led to development of numerous algorithms, comprehensively surveyed in [1]. Nevertheless, indoor localization still remains an open problem due to stringent requirements for high accuracy and low cost, demanded mostly from applications related to assisted living.

Due to its pervasive deployment and use, indoor localization built upon the exiting $2.4/5$ GHz WiFi infrastructure has been widely considered as an appealing cost-effective localization technology. In a prevailing fingerprinting approach, received signal strength (RSS) measurements from one or more access points (AP) are recorded at pre-determined locations in the offline stage, and a device is localized in an online stage by fusing online RSS measurements with those stored in the fingerprint database [3]. In an alternative, direct localization approach, a device is localized solely based on online WiFi RSS measurements, such that an often labor-intensive fingerprinting is avoided at the expense of deteriorated accuracy [2]. More recently, extraction of channel state information (CSI) from commercial IEEE 802.11n WiFi chipsets has become feasible and, thus, CSI fingerprinting with data-driven localization in the online stage has been studied [4].

To accommodate an ever increasing demand for data throughput, communication systems operating over millimeter-wave (mmWave) frequency ranges have started to emerge [5], [6]. Standards for indoor connectivity over unlicensed 60 GHz frequency range, such as IEEE 802.15.3c [7] and IEEE 802.11ad [8], have been around for some time. Envisioning that mmWave communications will become an ubiquitous technology, we study in this paper how future WiFi based on mmWave can be leveraged for indoor localization. More specifically, we propose a low-cost fingerprint-based localization method, where in addition to the RSS measurements we also fingerprint beam indices that two mmWave devices select from a finite set of feasible beams during their beam alignment procedure. The proposed method is experimentally evaluated using commercial off-the-shelf (COTS) IEEE 802.11ad-compliant 60 GHz routers and localization error of around 30 cm is achieved.

II. Relation to Prior Work

MMWave signals possess a certain set of features which make them highly suitable for indoor localization. First of all, mmWave signals experience relatively large propagation attenuation, especially pronounced at 60 GHz. On the other hand, small wavelengths enable packing a large number of antenna elements in relatively small form factors such that mmWave link between two devices is established using beamforming. In addition to the beamformed path, mmWave signal often propagates over few more paths, such that mmWave channel is sparse in the angular domain. In principle, the angular spectrum of mmWave channel between two devices can be directly mapped into location estimate of one device with respect to the other device, which has been utilized in [9]–

[12]. In an alternative approach, indoor localization based on mmWave channel fingerprinting has also been attempted. As such, [13] fingerprints RSS and angle of arrival (AoA) of mmWave signals transmitted from one or more APs. In a related work, [14] fingerprints high-resolution power delay profiles (PDP) over multiple beampatterns.

However, practical implementation of the above-referenced methods is challenging using current mmWave technology and communication standards. Namely, only a limited number of radio frequency (RF) chains are implemented into a mmWave transceiver due to hardware-related constraints. This precludes them from processing signals from all antenna elements in discrete-time domain and obtaining mmWave channel angular spectrum. Instead, a mmWave transceiver implements a finite number of possible beampatterns such that two mmWave devices establish communication link by probing different combinations of beams and choosing the one that yields the largest power in the received signal. In addition, even those limited channel measurements are not (easily) accessible from commercial mmWave chipsets which poses additional challenges to mmWave-aided localization.

We propose in this paper an indoor localization method based on fingerprinting measurements recorded during beam alignment stage and easily available from commercial chipsets. More specifically, we fingerprint RSS measurements and beam indices that two mmWave devices select from a finite set of feasible beams. Thus, in comparison to [13], [14], we are fingerprinting actual measurements that commercial mmWave devices record without requiring any hardware modifications. The closest work to this paper is [16], where SNRs over spatial beams measured during beam alignment procedures between commercial mmWave WiFi devices are extracted with the goal to directly estimate unknown location (i.e., without fingerprinting). In addition to extracting easily available RSS measurements and beam indices, our localization approach is based on fingerprinting, which yields more accurate location estimates even with fewer APs. This is more so when SNR measurements over spatial beams are fingerprinted, as done in our companion paper [17]. In addition to proposing a novel fingerprinting approach, we develop in this paper a method for extracting probabilistic models from the fingerprinted dataset and leveraging the models for online location estimation. Finally, we demonstrate the practical viability of the proposed method by implementing and experimentally testing it using our testbed comprising of commercially available 60 GHz off-the-shelf 802.11ad-compliant devices.

III. Proposed Localization Method

In this section, we describe the proposed localization method which comprises of offline, i.e., fingerprinting stage, and online, i.e., operational stage.

A. Localization Setup

Our indoor localization method is based on a fully opportunistic use of commercial off-the-shelf (COTS) mmWave WiFi routers. In particular, the proposed method leverages information about mmWave links established between a client and one or more APs that could be extracted from commercial transceiver chipsets. Towards that end, we utilize TP-Link Talon AD7200 router, which is one of the first and most popular WiFi 60 GHz devices complying with the IEEE 802.11ad standard. The TP link router implements Qualcomm QCA9500 transceiver that supports a single stream communication in 60 GHz range using analog beamforming over 32-element planar array. The TP-Link's transceiver receives in quasi-omnidirectional configuration and transmits by steering signal into one of 34 possible beams, realized using pre-stored beamforming weights. Notably, the resulting beams depart from the theoretical ones and exhibit fairly irregular shapes due to hardware imperfections at 60 GHz. As an example, Fig. 1 shows magnitudes of two transmit beams, experimentally measured in an anechoic chamber [16]. Two TP-Link devices establish mmWave communication link during beam alignment stage whereby one device is in the reception mode, i.e., implements quasi omni-directional beam, and measures the received signal levels of pilots sequentially transmitted over different beams by the other device. Upon this procedure, the two devices swap the roles the repeat the process. The beam alignment procedure yields beam indices to be used during data transmission, along with the RSS level measured over such a link. Following [15], we extract the recorded RSS and pair of transmit beam indices resulting from the TP-Link's beam alignment procedure and use that information for indoor localization. We emphasize that the developed algorithm can be generalized for the cases when mmWave transceivers employ different beam alignment procedures, for example when quasi-directional receive beams are also employed in addition to transmit beams.

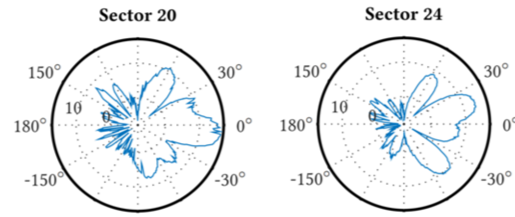

Fig. 1: Irregular beampatterns from TP-Link router [16].

B. Fingerprinting Stage

We assume K access points (AP), indexed $k = 1, \dots, K$, are deployed in an area of interest and their locations and orientations are fixed. An indoor area of interest is fingerprinted by a client device at different locations $l = 1, \dots, L$, such that the fingerprint measurements at each location are taken at different orientations of the client, indexed $o = 1, \dots, O$. The measurement record taken at a location-orientation pair (l, o) and corresponding to a mmWave link established with AP k is given as a set of triplets

$$\mathcal{D}_{l,o,k} = \left\{ \left(z_n, b_n^{(\mathrm{AP})}, b_n^{(\mathrm{C})} \right)_{n=1}^{N} \right\}, \quad (1)$$

where z_n is the received signal strength (RSS) measured over the link defined with beam indices $b_n^{(\mathrm{AP})}$ and $b_n^{(C)}$ that the AP k and client use for transmission. Without loss of generality, we assume the number of measurements N is the same irrespective of the location, orientation and AP. The overall measurement record corresponding to location-orientation pair (l, o) is

$$\mathcal{D}_{l,o} = \cup_{k=1}^{K} \mathcal{D}_{l,o,k} \tag{2}$$

As we have previously elaborated, the devices probe different beam pairs during the beam alignment stage of the mmWave protocol, and the pair of beams over which the training signal is received with the highest RSS level is the one used for information exchange. During the fingerprint stage, measurements of N such beam pairs, along with the corresponding RSS levels, are recorded by forcing the devices to perform beam alignment N times. Due to dynamics in the environment, the most prominent one being movement of people, the mmWave link measurements are not time-invariant. On the other hand, due to the directivity of mmWave channel, it is unlikely to observe N significantly different recordings of beam pairs. In particular, our measurements in an office space environment with a usual people traffic during regular business hours indicate that only several different beam pairs $(b^{(\mathrm{AP})}, b^{(\mathrm{C})})$ emerge over $N \sim 1000$ measurements.

Consequently, we summarize the measurement record $\mathcal{D}_{l,o,k}$ by clustering it into $J_{l,o,k}$ modes. Each mode is represented with a distinct pair $(b_j^{(\mathrm{AP})}, b_j^{(\mathrm{C})})$, $j = 1, \ldots, J_{l,o,k}$. The mode probability p_j is estimated as the relative frequency of occurrence of the beam pair representing mode j over the record of N measurements,

$$p_j = \frac{1}{N} \sum_{n=1}^{N} \mathbb{1}(b_j^{(\mathrm{AP})}, b_n^{(\mathrm{AP})}) \mathbb{1}(b_j^{(\mathrm{C})}, b_n^{(\mathrm{C})}), \tag{3}$$

where $\mathbb{1}(a, b) = 1$, if $a = b$, and zero, otherwise. Furthermore, the RSS levels measured for the same beam pair, i.e., mode, vary and thus each mode j is associated with a set of measured RSS levels $\mathcal{Z}_j$. This set is used to estimate mode probability distribution of RSS levels $p(z|j)$.

To estimate $p(z|j)$, the RSS level z is treated as a discrete random variable because commercial chipsets commonly measure it with a coarse quantization step, such as 1 dBm. Hence, $p(z|j)$ is the probability mass function directly estimated from the relative frequency of occurrence of RSS levels z in $\mathcal{Z}_j$. Due to silent fluctuations in mmWave channel and coarse quantization of RSS levels, it is not uncommon to observe previously unseen RSS levels over the link defining mode j that are thus not present in $\mathcal{Z}_j$. Therefore, $p(z|j)$ is estimated by accounting for that possibility such that

$$p(z|j) = \frac{1 + \sum_{\tilde{z} \in \mathcal{Z}_j} \mathbb{1}(\tilde{z}, z)}{|\mathcal{Z}_j| + m_j + 1}, \text{ if } z \in \mathcal{Z}_j \tag{4}$$

and

$$p(z|j) = \frac{1}{|\mathcal{Z}_j| + m_j + 1} \text{ if } z \notin \mathcal{Z}_j \tag{5}$$

where m_j denotes the number of different RSS levels in $\mathcal{Z}_j$, i.e., the alphabet size of the RSS levels. The adjustment of classical expressions for relative frequency of occurrence in (4) and (5) is motivated by the fact some RSS levels may not be well-represented in $\mathcal{Z}_j$, i.e., their number of occurrences is relatively small that the maximum likelihood (ML) estimate for the corresponding probability needs to be smoothed. In addition, a previously "unseen" RSS level may be measured in the online stage and thus we account for that situation by extending the RSS alphabet by one more element, corresponding to "unseen" RSS levels in the fingerprinting stage. The prior probability of occurrence of each element from such an alphabet is modelled as Dirichlet distribution with all hyper-parameters equal to one. The posterior probability of occurrence upon observing measurements from $\mathcal{Z}_j$ is evaluated according to (4) and (5), and often referred to as Laplace smoothing [18].

Overall, the fingerprint measurements $\mathcal{D}_{l,o,k}$ recorded at location l, with orientation o of the client device and corresponding to mmWave link with the AP k, is represented with the set of modes $\mathcal{S}_{l,o,k}$,

$$\mathcal{S}_{l,o,k} = \left\{ p_j, b_j^{(\mathrm{AP})}, b_j^{(\mathrm{C})}, p(z|j) \right\}_{j=1}^{J_{l,o,k}} \tag{6}$$

Analogously to (2), all mmWave link measurements taken at location l and orientation o of the client devices are summarized as

$$\mathcal{S}_{l,o} = \cup_{k=1}^{K} \mathcal{S}_{l,o,k} \tag{7}$$

Overall, the fingerprint database thus stores

$$\mathcal{S} = \cup_{l,o} \mathcal{S}_{l,o} \tag{8}$$

We note that the clustering approach considerably reduces the amount of memory required for storing fingerprint data. In addition, it streamlines the localization process in the online stage, as described in the following part.

C. Localization Stage

A client device is at unknown location and orientation in the environment and performs a cycle of beam alignments with all K APs sequentially before establishing a mmWave communication link with one of them. Without loss of generality, we assume the client performs I cycles of beam alignments with the APs. The measurements collected from AP k are represented as a set

$$\mathcal{M}_k = \left\{ (z_i, b_i^{(\mathrm{AP})}, b_i^{(\mathrm{C})})_{i=1}^{I} \right\} \tag{9}$$

The collection of measurements from all APs is

$$\mathcal{M} = \cup_{k=1}^{K} \mathcal{M}_k \tag{10}$$

We first consider the problem of detecting location l and orientation o represented in the fingerprint dataset, based on measurements $\mathcal{M}$ and fingerprint data $\mathcal{S}$. This is done by evaluating posterior distribution of (l, o) given measured and training data, which is using Bayes' rule expressed as

$$p(l, o|\mathcal{M}, \mathcal{S}) \propto p(\mathcal{M}|l, o, \mathcal{S})\, p(l, o) \tag{11}$$

where $l = 1, \ldots, L$, $o = 1, \ldots, O$. The prior distribution of the client $p(l, o)$ is assumed uniform over the space of possible (l, o). We note that in device tracking problem, $p(l, o)$ encodes prior information of client's position based on previous position estimate and odometry measurements. Since the set of location-orientation pairs (l, o) is finite, the normalization constant in (11) is not explicitly computed.

Assuming independent measurements across APs and time, the likelihood term from (11) is given by

$$\begin{aligned} p(\mathcal{M}|l, o, \mathcal{S}) &= p(\mathcal{M}|\mathcal{S}_{l,o}) = \prod_{k=1}^{K} p(\mathcal{M}_k|\mathcal{S}_{l,o,k}) \\ &= \prod_{k=1}^{K} \prod_{i=1}^{I} p(z_i, b_i^{(\mathrm{AP})}, b_i^{(\mathrm{C})}|\mathcal{S}_{l,o,k}) \quad (12) \end{aligned}$$

The conditional probability of a measurement triplet in (12) is evaluated assuming independence of the RSS level from the beam indices, as well as the independence of the beam indices,

$$\begin{aligned} & p(z_i, b_i^{(\mathrm{AP})}, b_i^{(\mathrm{C})}|\mathcal{S}_{l,o,k}) = \\ & \textstyle\sum_{j=1}^{J_{l,o,k}} p_j \; p(z_i|j) \; p(b_i^{(\mathrm{AP})}|b_j^{(\mathrm{AP})}) \; p(b_i^{(\mathrm{C})}|b_j^{(\mathrm{C})}) \qquad (13) \end{aligned}$$

where p_j, $b_j^{(\mathrm{AP})}$, $b_j^{(\mathrm{C})}$ and $p(z|j)$ are, respectively, the probability, AP's beam index, client's beam index and RSS distribution representing mode j of $\mathcal{S}_{l,o,k}$ from (6).

We consider two approaches in specifying the conditional probabilities $p(b_i^{(\mathrm{AP})}|b_j^{(\mathrm{AP})})$ and $p(b_i^{(\mathrm{C})}|b_j^{(\mathrm{C})})$. Noting that the functional form of those distributions is the same irrespective of the device type, AP or client, we omit the superscript and denote with $p(b_i|b_j)$ the conditional probability that beam alignment procedure suggests beam index b_i for transmission when the device is in the mode represented by beam index b_j. In a hard approach,

$$p(b_i|b_j) = \mathbb{1}(b_i, b_j) \qquad (14)$$

More specifically, this approach excludes the possibility that the suggested beam index is different from the one representing a mode. In other words, if a client and AP negotiate a pair of beam indices that is not present in the fingerprint dataset at a certain location and orientation, the model (14) assigns zero posterior probability that the client is at that particular location and orientation. This approach is justified when the beampatterns corresponding to beam indices are orthogonal, or sufficiently large number of measurements at each location-orientation (l, o) is recorded. However, the beampatterns of the COTS mmWave WiFi routers are considerably deviating from the theoretical ones, let alone orthogonal, as illustrated in Fig. 1. As a result, a link between AP and client over a certain channel path can often be established with more than one possible pair of beam indices. For example, assume AP and client communicate over $(b_1^{(\mathrm{AP})}, b^{(\mathrm{C})})$ and $(b_2^{(\mathrm{AP})}, b^{(\mathrm{C})})$ equally well, i.e., with the same RSS level, and that the beampatterns corresponding to $b_1^{(\mathrm{AP})}$ and $b_2^{(\mathrm{AP})}$ are quite similar, which is not uncommon in COTS devices. Thus, if $(b_1^{(\mathrm{AP})}, b^{(\mathrm{C})})$ is present in the fingerprint dataset and $(b_2^{(\mathrm{AP})}, b^{(\mathrm{C})})$ is measured in the localization stage at the same location and orientation (l, o), the hard model (14) would assign zero probability that the client is at (l, o). To avoid such an issue, a softer approach in modeling $p(b_i|b_j)$ is needed.

Since the beampatterns of COTS devices can be measured and are available, we model the conditional beam probability $p(b_i|b_j)$ with a cross-correlation between the corresponding beampattens' magnitudes,

$$p(b_i|b_j) = \frac{\mathbf{b}_i^T \mathbf{b}_j}{\sum_{p=1}^{P} \mathbf{b}_p^T \mathbf{b}_j}, \; i = 1, \ldots, P \qquad (15)$$

where $\mathbf{b}_i$ and $\mathbf{b}_j$ are vector representations of the magnitudes of beampatterns indexed with b_i and b_j, and P is the number of different beampatterns implemented in the used COTS devices. Therefore, the soft beam probability model (15) assigns relatively high probability to all beampatterns that are similar to the one indexed by b_j. Back to our simple example, even though the measured beam index $b_1^{(\mathrm{AP})}$ is different from the one recorded in the fingerprint dataset, $b_2^{(\mathrm{AP})}$, the fact their corresponding beampatterns are similar yields relatively high beam probability $p(b_1^{(\mathrm{AP})}|b_2^{(\mathrm{AP})})$, thus giving the algorithm chance to detect that the client is at correct location and orientation (l, o).

Finally, substituting (15) into (13), and the result into (12) yields the likelihood of test measurements $\mathcal{M}$ at a location-orientation pair (l, o). This likelihood is substituted into (11), together with possibly non-uniform prior $p(l, o)$, to eventually yield (after normalization) the posterior distribution of location-orientation pairs. The client's location and orientation are detected based on its measurements $\mathcal{M}$ as the location-orientation pair with the largest posterior probability,

$$\hat{l}, \hat{o} = \arg\max_{l,o} p(l, o|\mathcal{M}, \mathcal{S}) \qquad (16)$$

Commonly, unknown location and orientation of the device are not the ones at which fingerprint data is collected. Therefore, we estimate the client's location and orientation as centroids of locations and orientations at which fingerprint data is collected, with weights equal to the posterior probabilities (11). More formally, denoting the vector of Cartesian coordinates corresponding to location indexed with l as $\mathbf{r}_l$ and the orientation indexed with o as θ_o, the unknown client's position and orientation are estimated as

$$[\hat{\mathbf{r}} \quad \hat{\theta}] = \sum_{l,o} p(l, o|\mathcal{M}, \mathcal{S}) \; [\mathbf{r}_l \quad \theta_o] \qquad (17)$$

When the client's Cartesian coordinates are only of interest, which is often the case, their vector representation is estimated as

$$\hat{\mathbf{r}} = \sum_{l} p(l|\mathcal{M}, \mathcal{S}) \; \mathbf{r}_l, \qquad (18)$$

where the posterior probability of locations is given by $p(l|\mathcal{M}, \mathcal{S}) = \sum_o p(l, o|\mathcal{M}, \mathcal{S})$.

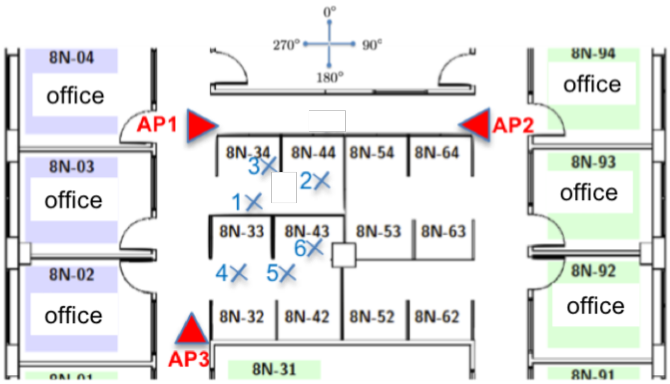

Fig. 2: Floor plan of the indoor area.

IV. Experimental Evaluation

The proposed localization approach and algorithm are tested in an indoor office space, whose floor plan is shown in Fig. 2. The indoor area consists of offices, separated from hallway by wooden doors, concrete wall and glass windows, as well as of cubicles separated by typical partitions. More details on the indoor area can be seen in Fig. 3. We deploy four TP-Link routers in the indoor area. Three routers are designated as access points (AP) and their locations and orientations are fixed, while the remaining router acts as a client and is moved throughout the indoor area. The indoor area is fingerprinted at $L = 6$ locations, with $O = 4$ possible orientations at each location, where $\theta = \{0, 90°, 180°, 270°\}$, yielding overall 24 location-orientation pairs. All fingerprint and tests measurements are taken during business hours with regular traffic of people, including opening and closing of doors, people passing by, small groups of people standing in different areas of the space for some, usually short, amount of time. The positions of APs (red triangles) and fingerprint locations (blue crosses labeled with numbers) are shown in Fig. 2. Referring to Figures 2 and 3, the separation between AP1 and AP2 is 2.95 m, while that of AP1 and AP3 is 2.26 m. The distance between fingerprint locations ranges between 0.4 m and 1.28 m, with the mean value of 0.82 m.

As discussed, a location-orientation pair is fingerprinted with measurements of RSS and indices of transmit beams yielded from the beam alignment stage with each of the three APs. We emphasize that the RSS measurements extracted from the COTS routers are coarsely quantized with 1 dBm quantization step. The number of measurements taken at different location-orientation settings is between 1000 and 3000. An example of measurements at $l = 6$ and $o = 1$ ($\theta = 0°$) recorded during the establishment of a link with AP3 is shown in Fig. 4. As can be seen, the beam indices exhibit a low-to-moderate variability, while the RSS varies within 10 dB over the measurement window.

To evaluate the localization performance, we take test measurements of RSS and beam indices at three test locations, labeled A, B and C, at all four considered orientations. The test measurements are taken several months after fingerprinting.

Fig. 3: Pictures of the indoor area.

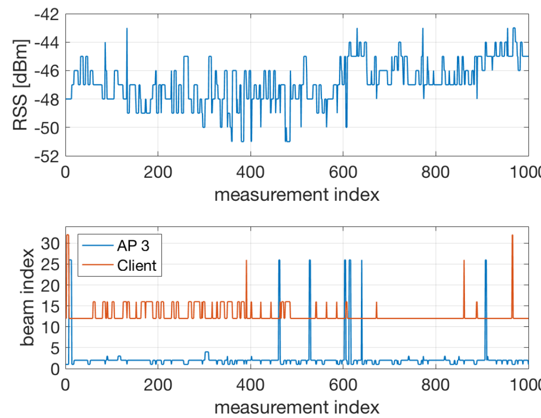

Fig. 4: Link measurements at $l = 6$, $o = 1$ ($\theta = 0°$) to AP3.

The relative positions of the fingerprint (FP) and test locations are shown in Fig. 5. Notably, the average distance of the test locations from the fingerprint locations is 60 cm. The number of measurements taken at a test location and each of four orientations is summarized in Table I.

Although a test measurement at a test location is taken by pointing the client towards one of four orientations, our goal is to estimate location of the device. Consequently, the proposed method estimates the coordinates of the unknown location by essentially integrating over orientations represented in the fingerprint dataset, as suggested by (18). It is worth pointing out that device's orientation could also be estimated using

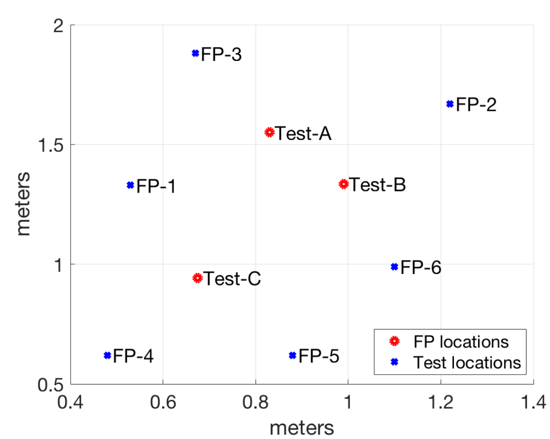

Fig. 5: Coordinates of fingerprint (FP) and test locations.

TABLE I: Number of test measurements

Test location	0°	90°	180°	270°	All
A	949	1326	1887	2034	6169
B	1712	1533	1469	1304	6018
C	1399	2426	2427	2403	8655

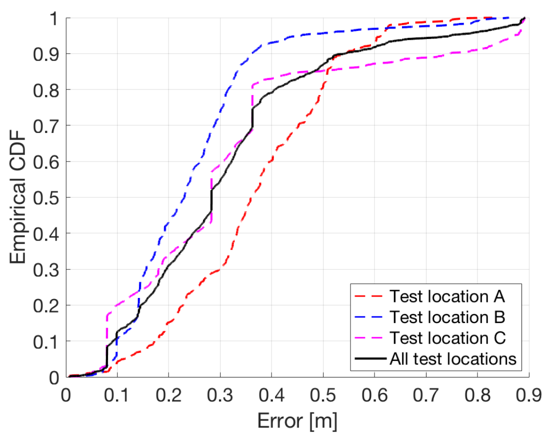

Fig. 6: Empirical CDF of localization errors at test locations.

the proposed algorithm, provided that fingerprint dataset is recorded with finer orientation resolution.

The localization algorithm employs soft beam model (15) and is supplied with one measurement triplet consisting of RSS and beam indices corresponding to each of three APs, i.e., $I = 1$. The localization error, measured as the distance between the estimated and ground-truth locations, is used as a performance metric. The empirical cumulative distribution function (CDF) of localization errors measured at each of the three test locations separately, as well as across all test locations, is shown in Fig. 6. The mean and median localization errors achieved at each and across all test locations are summarized in Table II. Overall, the proposed algorithm achieves around 30 cm error in estimating unknown locations whose average distance from the fingerprint locations is 60 cm. In comparison to our companion paper [17] which fingerprints SNR measurements across all beams with resulting localization accuracy of 17.5 cm, the method in this paper fingerprints smaller amount of measurements, more easily available from the COTS devices, and at coarser quantization level.

V. Conclusions

We presented in this paper an indoor localization method based on a fully opportunistic use of commercial mmWave WiFi routers. The proposed method fingerprints transmit beam indices used by a pair of WiFi devices to establish mmWave communication link, as well as the RSS associated with that link. Notably, this information is relatively easily available from commercial WiFi transceivers. We developed an algorithm that learns possible probabilistic modes from the fingerprint data and leverages those modes for estimating unknown location in the online stage. The developed method is experimentally validated using four commercially

TABLE II: Mean and median of test localization errors

Test location	A	B	C	All
Mean error [m]	0.3654	0.2428	0.3144	0.3089
Median error [m]	0.3609	0.2306	0.2831	0.2831

available 60 GHz TP-Link routers complying with the IEEE 802.11ad standard operating over 60 GHz and localization error $\sim$ 30 cm is demonstrated.

References

[1] Y. Gu, A. Lo, and I. Niemegeers, “A survey of indoor positioning systems for wireless personal networks,” *Communications Surveys Tutorials, IEEE*, vol. 11, no. 1, pp. 13–32, First quarter 2009.

[2] M. Pajovic, P. Orlik, T. Koike-Akino, K. J. Kim, H. Aikawa and T. Hori, “An unsupervised indoor localization method based on received signal strength (RSS) measurements,” in *Proc. Global Communications Conference (GLOBECOM)*, San Diego, CA, USA, pp. 1-6., Dec. 2015.

[3] T. King, S. Kopf, T. Haenselmann, C. Lubberger, and W. Effelsberg, “COMPASS: A probabilistic indoor positioning system based on 802.11 and digital compasses,” in *Proc. First ACM Intl Workshop on Wireless Network Testbeds, Experimental evaluation and Characterization (WiNTECH)*, Los Angeles, CA, USA, Sept. 2006.

[4] X. Wang, L. Gao, S. Mao, and S. Pandey, “CSI-based fingerprinting for indoor localization: A deep learning approach,” *IEEE Trans. Veh. Technol.*, vol. 66, no. 1, pp. 763–776, Jan. 2017.

[5] T. S. Rappaport, S. Sun, R. Mayzus, H. Zhao, Y. Azar, K. Wang, G. N. Wong, J. K. Schulz, M. Samimi and F. Gutierrez, “Millimeter wave mobile communications for 5G cellular: It will work!," in *IEEE Access*, vol. 1, pp. 335–349, 2013.

[6] T. S. Rappaport, R. W. Heath, R. C. Daniels and J. N. Murdock, “Millimeter wave wireless communications," in *Pearson Education*, 2014.

[7] “IEEE standards 802.15.3c-2009: Millimeter-wave-based alternate physical layer extension," IEEE Standards Association., 2009.

[8] “IEEE standards 802.11ad-2012: Enhancements for very high throughput in the 60 GHz band," IEEE Standards Association., 2012.

[9] F. Lemic et al., “Localization as a feature of mmWave communication," in *Proc. of International Wireless Communications and Mobile Computing Conference (IWCMC)*, Paphos, 2016, pp. 1033–1038.

[10] J. Chen, D. Steinmetzer, J. Classen, E. Knightly and M. Hollick, “Pseudo lateration: Millimeter-wave localization using a single RF chain," in *Proc. of IEEE Wireless Communications and Networking Conference (WCNC)*, San Francisco, CA, USA, pp. 1–6., 2017.

[11] A. Olivier, G. Bielsa, I. Tejado, M. Zorzi, J. Widmer and P. Casari, “Lightweight indoor localization for 60-GHz millimeter wave systems," in *Proc. of 13th Annual IEEE International Conference on Sensing, Communication, and Networking (SECON)*, London, pp. 1–9., 2016.

[12] J. Palacios, P. Casari and J. Widmer, “JADE: Zero-knowledge device localization and environment mapping for millimeter wave systems," in *Proc. of IEEE Conference on Computer Communications (INFOCOM)*, Atlanta, GA, USA, pp. 1–9., 2017.

[13] Z. Wei, Y. Zhao, X. Liu and Z. Feng, “DoA-LF: A location fingerprint positioning algorithm with millimeter-wave," in *IEEE Access*, vol. 5, pp. 22678–22688, 2017.

[14] J. Gante, G. Falcao and L. Sousa, “Beamformed fingerprint learning for accurate millimeter wave positioning", in *VTC Fall*, pp. 1–5., Aug. 2018.

[15] D. Steinmetzer, D. Wegemer, and M. Hollick. (2017) “Talon tools: The framework for practical IEEE 802.11ad research," [Online] Available: https://seemoo.de/talon-tools/

[16] G. Bielsa, J. Palacios, A. Loch, D. Steinmetzer, P. Casari and J. Widmer, “Indoor localization using commercial off-the-shelf 60 GHz access points," in *IEEE INFOCOM*, pp. 2384-2392., April 2018.

[17] P. Wang, M. Pajovic, T. Koike-Akino, H. Sun, and P. V. Orlik, “Fingerprinting-based indoor localization with commercial mmWave WiFi routers - Part II: Spatial beam SNRs," in *IEEE Global Communications Conference (GLOBECOM)*, Waikoloa, HI, USA, Dec. 2019.

[18] C. M. Bishop, “Pattern Recognition and Machine Learning (Information Science and Statistics)", Springer-Verlag, 2006.